On Buckling Accepted Design of Ship Structures Utilizing High Tensile Steels†

Yukio UEDA*, Sherif M. H. RASHED** and Yehia Abdel-NASSER***

Abstract

Among the trends of revolution for ship structures, the use of high tensile steels in many parts of the structures has been tried by many arganizations concerned. With high tensile steels, ship structures will be generally thinner than those with conventional mild steel, taking account of higher yield strength of the material. This, in turn, will lead to lower buckling strength. This fact may suggest to accept buckling of such structures in order to utilize the advantage of high yield strength of the material.

Allowing buckling in ship structures will bring out several problems. This paper dicusses some of these problems, namely: the maximum stress, ultimate stength and fatigue strength under regular and random loads. A design philosophy on buckling accepted design is proposed. Design criteria, design methods and related design graphs are presented in connection with the new design philosophy.

KEY WORDS: (Buckling accepted design) (Flat plate) (Maximum stress) (Ultimate strength) (Fatigue strength) (High tensile strength steel)

1. Introduction

Among the trends of revolution in the shipbuilding industry, high tensile steel is considered for sue in many parts of ship structures. Lighter scantlings are expected utilizing effectively the high yield stress of this material. Such lighter scantlings may be lower in buckling strength than those of ship structures built using conventional mild steel. From practical viewpoint against improvement of buckling strength, reducing stiffener spacing in proportion to the high yield stress is not an efficient way. This suggests an alternate way that buckling should be accepted in ship structures if the high yield strength of the material is aimed to be utilized.

Buckling in ship structures may be classified into column buckling, stiffened panel buckling and buckling of primary supporting members. Column buckling (flexural, torsional or lateral) leads to collapse of the column with ultimate strength which is almost equal to the buckling strength. No benefits may be obtained to use higher strength steels.

Buckling of stiffened plates may take place in several different modes.

a) Overall buckling: In this mode of buckling, plate panels and stiffeners comprising a stiffened plate bounded by four primary supporting members, such as bulkheads or strong girders and stringers, buckle together. This kind of buckling usually leads to collapse of the whole plate of which carrying capacity is lower than that at local buckling and must not be allowed.
b) Stiffeners lateral buckling: This mode of buckling usually leads to overall buckling and collapse of the stiffened plate. Such practice as avoiding this mode of buckling is usually provided.
c) Local buckling of plate panels between stiffeners: Plate panels may buckle but still continue to carry substantial further load after buckling as long as its edges continues to be effectively supported by the stiffeners. This mode of buckling may be allowed to exploit the high yield stress of the material.

Primary supporting members, such as deck and bottom girders may buckle in three different modes.

a) Lateral buckling: The carrying capacity of a girder is mainly governed by this mode of buckling and nothing can be gained by allowing this mode of buckling.
b) Torsional buckling of the flange: This usually leads to lateral buckling and should not be allowed.
c) Web bukling: In stiffened web plates, only plate panels between stiffeners may be allowed to buckle.

From the above discussion, it may be seen that only effectively supported plate panels may be allowed to buckle in order to exploit the advantage of high tensile steels.

† Received on May 6, 1992
* Director professor
** Technical Manager, MSC Japan Ltd.
*** Graduate Student, Osaka University

Transactions of JWRI is published by Welding Research Institute of Osaka University, Ibaraki, Osaka 567, Japan

These plate panels, however, may constitute about 80 % of the ship hull weight and substantial economic benifits may be gained by reducing the thickness of these plate panels.

Allowing buckling in ship structures will bring out several problems. Three subjects related to rectangular plate panels subjected to uniaxial compression are discussed in this paper, namely, the maximum stress, ultimate strength, fatigue strength under regular and random loads.

A design philosophy on buckling accepted design is proposed, and design criteria, methods and graphs are presented in connection with these subjects.

2. Consequences of plate buckling in ship structures

Let's consider a flat stiffened plate, as shown in **Fig. 1**, free of any imperfections such as initial deflection or/and welding residual stresses, and simply supported at its edges. It is assumed that the plate thickness is such that it will buckle in an early loading stage, and the stiffeners be such that they will not buckle or collapse before the plate panels have reached their ultimate strength. The edges are assumed to be kept straight but free to move in the plane of the plate.

For simplicity of discussion, the panel is supposed to be subjected to an increasing uniaxial inplane compression in the direction of the stiffeners. The arguments to be mentioned here should be valid, however, for other combined loading conditions. As the load increases starting from zero, a linear (uniform) stress distribution develops across the breadth. When the load reaches the critical load, plate panels buckle, and buckling deflection is induced in the following patterns characterized as,

a) each half buckling wave tends to have a length close to stiffener spacing,
b) buckling deflection of adjacent plates is produced usually in opposite directions as shown in Fig. 1.

This phenomena resembles buckling of simply supported plate panels, except the restraint provided by the torsional stiffness of the stiffeners, and the webs of the primary supporting members around the stiffened plate.

With further loading, buckling deflection increases. This leads to a more complicated stress distribution as shown in **Fig. 2**. Four important consequences of this stress distribution are:

1) maximum(locally maximum) stresses higher than the nominal (average) stress are developed. These may occur at the edges or at the central portions of each half buckling waves on the concaved surface.
2) ultimate strength becomes smaller than the fully plastic strength which the plate could have attained if buckling did not occur. The smaller the ratio σ_{cr}/σ_o is, the smaller is P_u/P_o where,

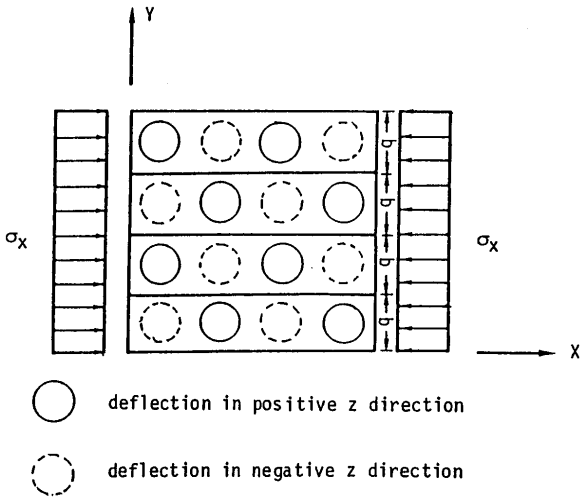

Fig. 1 Stiffened panel and considered buckling mode

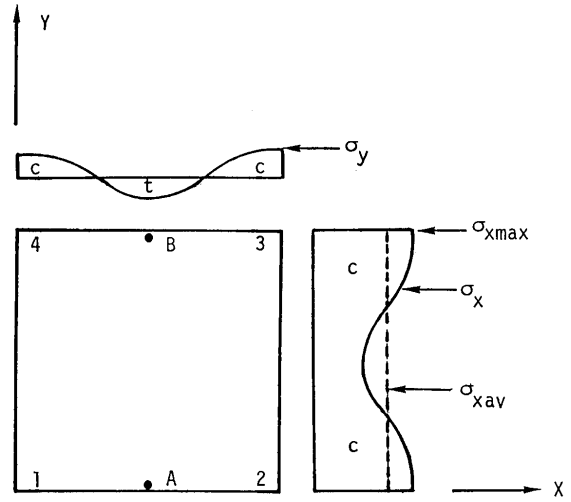

Fig. 2 Stress distribution in a buckled plate

σ_{cr} = critical(buckling) stress of the plate fields
σ_o = yield stress of the material
P_u = plate ultimate strength
P_o = plate fully plastic strength

3) complicated 3-dimensional stress distribution is developed in the vicinity of welds between the stiffeners and panels. This is due to plate buckling restrained by the torsional stiffness of the stiffeneers.
4) Tangential stiffness of the buckled plated is reduced to about 0.5 of its original one.

The first of these consequences should be discussed with respect to the allowable maximum stress design criterion which is used with conventional design loads. The second is related to safety evaluation in extreme loading conditions. The third is related to fatigue strength and the fourth is concerned with the stiffness of ship hull in response to different loading conditions.

In the following sections, the first three consequences are discussed.

3. Design philosophy

Traditionally ship structures are designed based on rules developed from the past experience. Although the concept of design by analysis has been popular for quite some time, it has been applied only partially in some ship hull designs such as LNG carriers. To the knowledge of the authors, there is only one design[1)] which is fully carried out according to this concept. In this design, selected factors of safety, allowable stresses, safety criteria etc., are based on the past experience. This is natural because it is only rational to have utilized the experience accumulated during hundreds of years of shipbuilding and operation. Although the authors are in favour of the idea of design by analysis, until some absolute design criteria for all possible loading conditions could be established, design should be carried out "In comparison with present ships with satisfactory performances" or "in reference to conventional design rules as an average of the present practice."

In ship structures, however, fatigue strength is substantially influenced by many factors such as (1) the type of ship (2) types and locations of individual members even in the same ship and (3) the kind of used steels. Therefore, the design for fatigue strength needs an absolute values of criteria and accurate evaluation of actual fluctuating stresses based on experimental studies and experience which have been gained in the design of offshore structures.

For the use of high tensile steels for plate panels in ship hulls, taking account of this discussion and considering the consequences of plate buckling mentioned in the preceding section, the following criteria should be added to the conventional ones, if the buckling accepted design is applied to plate panels in ship hulls.

1. Maximum stress criterion: Maximum stress anywhere in the plating or the attached stiffeners should not exceed the yield stress divided by a factor of safety which is equal to that used with ship hulls built with conventional mild stee. i.e.

$$\sigma_{max} \leqq \sigma_o/f_s$$

where, σ_{max} = maximum stress in the buckled plate or attached stiffeners,
f_s = a suitable factor of safety based on present experience.

2. Ultimate strength: Ultimate strength of a high tensile steel plate panels should be equal to or greater than that of a corresponding conventional mild steel plate i.e.

$$P_{UHTS} \geqq P_{USS}$$

where, P_{UHTS} = ultimate stength of a high tensile steel plate panel
P_{USS} = ultimate strength of a corresponding conventional steel plate panel.

A corresponding conventional steel plate panel is defined as a conventional steel plate designed to carry the same design load according to the maximum stress criteria in 1. above.

3. Fatigue strength: Alternating random stresses are to be limited to the values corresponding to the required fatigue life. In other words, the calculated fatigue life should be more than or equal to the required fatigue life (in ship structures, fatigue life is usually taken as 10^8 cycles) i.e.

$$N_c \geqq N_r$$

where, N_c = calculated fatigue life
N_r = required fatigue life

These criteria will be discussed in details in sections 4, 5 and 6.

4. Design against maximum stress

The same stiffened plate as shown in Fig. 1 is considered, assuming the attached stiffeners will not fail before the plate panels reach their ultimate strength.

The buckling strength of the plate panels may be expressed as follows.

$$\sigma_{xcr} = k \frac{\pi^2 E}{12(1-\nu^2)} (t/b)^2 \tag{1}$$

where, E is the Young'modulus
and, ν is the Possion's ratio
for long plates k may be taken equal to 4.

With loads higher than the buckling load, the stress distribution becomes as shown in Fig. 2. Maximum membrane stress σ_{xmax} (compression) in x direction occurs along the longitudinal edges of the plates while the minimum membrane stress σ_{ymin} (tension) in y direction occurs in the middle of each half buckling wave. If the aspect ratio of one half wave is assumed to be 1.0, σ_{xmax} and σ_{ymin} may be expressed as follows.

$$\sigma_{xmax} = 2\,\sigma_{xav} - \sigma_{xcr} \tag{2}$$

$$\sigma_{ymin} = -\sigma_{xav} + \sigma_{xcr} \tag{3}$$

On the concave surface of the panel on the central portion of each half buckling wave, bending stress is superimposed on the membrane stress. However, bending stress is not considered in this study for two reason.

1. For thin plates, which are the main interest of this study, this surface stress is smaller than the edge membrane stress.

2. Even for thicker plates this surface stress is not a direct cause of collapse.

Since the stiffeners are assumed not to fail before the plate panel does, the stress in the stiffeners will always be smaller than the maximum equivalent stress in the buckled plate with respect to the yield condition. Only the maximum membrane equivalent stress of the plate at the edges is considered here.

Maximum equivalent stress occurs where σ_x is maximum (in compression) and σ_y is minimum(in tension), i.e. in the middle of individual half budkling waves along the longitudinal edges and may be expressed as follows.

$$\sigma_{VM}{}^2 = \sigma^2{}_{xmax} + \sigma^2{}_{ymin} - \sigma_{xmax}\sigma_{ymin} + 3\tau^2{}_{xy} \quad (4)$$

Substituting Eqs. (2) and (3) into Eq. (4) and imposing the condition that σ_{VM} be equal to the allowable stress σ_{all}, a design limit may be obtained as follows.

$$\sigma_{all}{}^2 = 7\sigma_{xav}{}^2 - 9\sigma_{xav}\sigma_{xcr} + 3\sigma_{xcr}{}^2 \quad (5)$$

Solving this equation for σ_{xav}, choosing the correct solution and dividing by σ_{all},

$$\frac{\sigma_{xav}}{\sigma_{all}} = (1/14)\left[9\frac{\sigma_{xcr}}{\sigma_{all}} + \left(-3\frac{\sigma_{xcr}{}^2}{\sigma_{all}{}^2} + 28\right)^{1/2}\right] \quad (6)$$

Substituting Eq. (1) into Eq. (6), a relation between the highest allowable average stress σ_{xav} and b/t may be obtained as,

$$\frac{\sigma_{xav}}{\sigma_{all}} = (1/14)\left\{\frac{9c}{\beta_a{}^2} + \left(-3\left[\frac{c}{\beta_a{}^2}\right]^2 + 28\right)^{1/2}\right\} \quad (7)$$

where, $\beta_a = b/t(\sigma_{all}/E)^{1/2}$,

$c = k\,\pi^2/[12(1-\nu^2)]$

Equation (7) may be plotted as indicated in **Fig. 3**.

Equation (7) or Fig. 3 may be used ot evaluate the allowable average stress σ_{xav}, to be applied on a plate when b/t, E (Young's modulus) and the allowable stress, σ_{all}, for the specified material are known.

Here, several cases of the panel shown in Fig. 1 are considered. The standard case is a conventional mild steel plate with σ_{all} = 15kgf/mm² (σ_o = 30 kgf/mm², the factor of safety f_s=2). In the other case, the plate is replaced by various high tensile steel plates. Using Eq. (7), **Fig. 4** shows the maximum allowable average stress for plates with different thicknesses made of high tensile steel with allowable stress equal to 25 kgf/mm² (σ_o = 50 kgf/mm², the

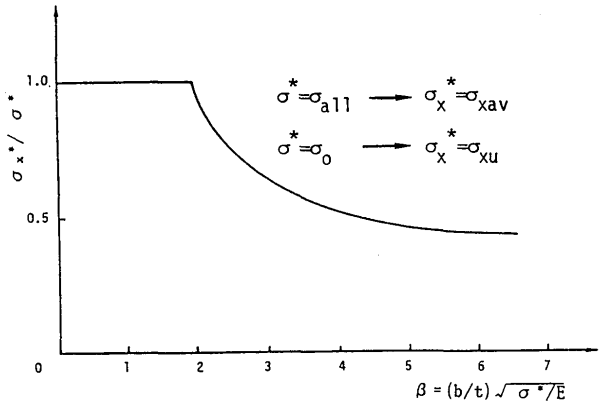

Fig. 3 Relationships of maximum allowable average stress and ultimate average stress to plate slenderness ratio β

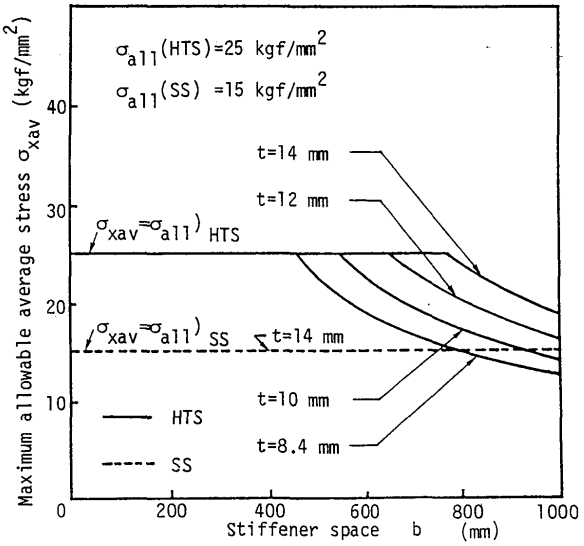

Fig. 4 Relationships of maximum allowable average stress to stiffener space

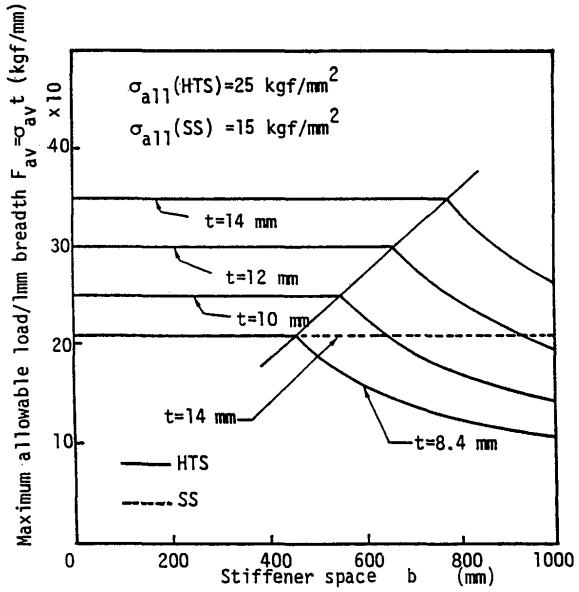

Fig. 5 Relationships of maximum allowable load to stiffener space

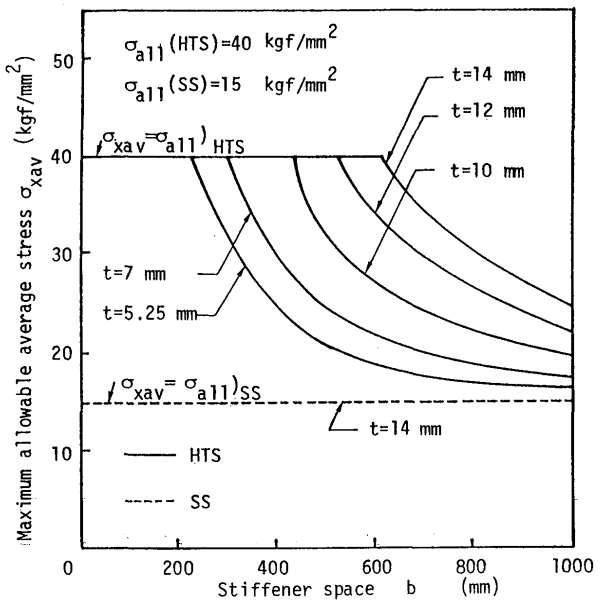

Fig. 6 Relationships of maximum allowable average stress to stiffener space

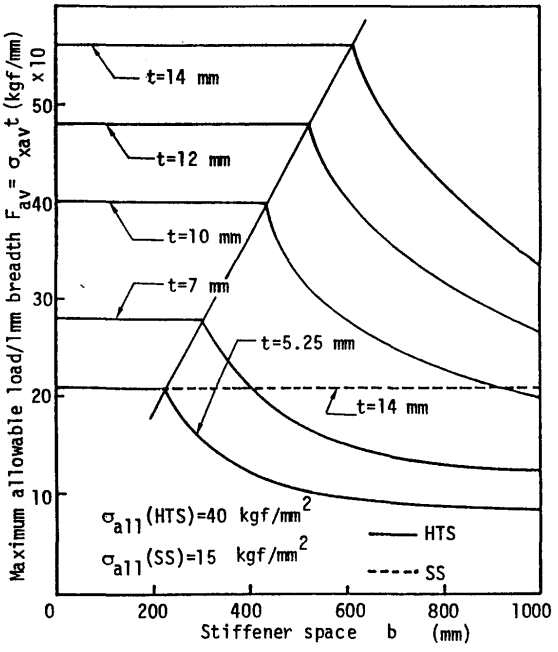

Fig. 7 Relationships of maximum allowable load to stiffener space

factor of safety $f_s=2$) plotted against the stiffener spacing. **Figure 5** shows the maximum allowable load per unit breadth ($\sigma_{av}t$) of these plates also plotted against the stiffener spacing. These figures indicate the possible reduction of plate thickness which may be achieved by adopting such a high tensile steel. For example, with a fixed frame spacing equal to 900 mm, reduction of plate thickness by 2 mm may be achieved while maintaining the same load as that carried by the conventional mild steel plate of 14 mm in thickness. With a frame spacing of 700 mm, a high tensile steel plate 10.5 mm thick may be used to carry the same load as that carried by the original plate. Similar relationships for σ_{all} = 40 kgf/mm² (σ_o = 80 kgf/mm², $f_s=2$) are shown in **Figs. 6** and **7**.

It is to be noted here that plates 8.4 mm thick with stiffener spacing of 460 mm, and 5.25 mm thick with stiffener spacing of 225 mm may be used in cases of σ_{all} = 25 kgf/mm² and 40 kgf/mm² respectively, if buckling is prevented, while carrying the same load as the original steel plate of 14 mm in thickness.

5. Design against ultimate strength

For the stiffened plate in Fig. 1, the ultimate strength after plate panels have buckled, may be accurately estimated by assuming that the ultimate strength state is reached when the yield condition (Von Mises'condition in this paper) is satisfied in the middle of a half buckling wave along the longitudinal edges[2]. As mentioned in section 4, at such location, σ_x is maximum(compression) and σ_y is minimum(tension), which may still be expressed by Eqs. (2) and (3), and the Von Mises yield condition may be expressed as follows,

$$\sigma_o^2 = \sigma^2_x + \sigma^2_y - \sigma_x\sigma_y + 3\tau^2_{xy} \tag{8}$$

Substituting Eqs. (1), (2) and (3) into Eq. (8) and noting that the average stress σ_{xav} in this case equals to the ultimate average stress σ_{xu}, an equation similar to Eq. (7) may be obtained in which σ_o replaces σ_{all} and σ_{xu} replaces σ_{xav}.

$$\frac{\sigma_{xu}}{\sigma_o}=(1/14)\{\frac{9c}{\beta^2}+(-3[\frac{c}{\beta^2}]^2+28)^{1/2}\} \tag{9}$$

where, $\beta=b/t(\sigma_o/E)^{1/2}$

Equation (9) may be represented by the same curve in Fig. 3.

Writing Eq. (9) for a conventional mild steel panel and a high tensile steel panel, using subscripts ss and HTS for these steels,

$$\frac{\sigma_{xuss}}{\sigma_{oss}}=(1/14)\{\frac{9c}{\beta_s^2}+(-3[\frac{c}{\beta_s^2}]^2+28)^{1/2}\} \tag{10}$$

where, $\beta_s=b/t(\sigma_{oss}/E)^{1/2}$

$$\frac{\sigma_{xuHTS}}{\sigma_{oHTS}}=(1/14)\{\frac{9c}{\beta_h^2}+(-3[\frac{c}{\beta_h^2}]^2+28)^{1/2}\} \tag{11}$$

where, $\beta_h=(b/t)\ (\sigma_{oHTS}/E)^{1/2}$

Dividing Eq.(11) by Eq. (10), the $\sigma_{xuHTS}/\sigma_{xuss}$ may be expressed as follows

$$\frac{\sigma_{xuHTS}}{\sigma_{xuss}} = \frac{(t/b)_{HTS}^{\ 2}}{(t/b)_{ss}^{\ 2}} \frac{\{1+(1/9)[-3+28(\beta_h^2/c)^2]^{1/2}\}}{\{1+(1/9)[-3+28(\beta_s^2/c)^2]^{1/2}\}} \quad (12)$$

The condition for equal ultimate strength (N_{XU}) of both plates may be expressed as follows,

$$\frac{N_{xuHTS}}{N_{xuss}} = \frac{\sigma_{xuHTS}\, t_{HTS}}{\sigma_{xuss} t_{ss}} = 1 \quad (13)$$

i.e.

$$\frac{t_{HTS}}{t_{ss}} \cdot \frac{(t/b)_{HTS}^{\ 2}}{(t/b)_{ss}^{\ 2}} \frac{\{1+(1/9)[-3+28(\beta_h^2/c)^2]^{1/2}\}}{\{1+(1/9)[-3+28(\beta_s^2/c)^2]^{1/2}\}} = 1 \quad (14)$$

Equation (14) gives the relationship between the thickness of a conventional mild steel plate and that of a high tensile steel plate for the same ultimate strength.

The design concept against ultimate strength is applied to the same panel of Fig. 1 using high tensile steel. **Figure 8** represents the average ultimate stress σ_{xu} of plates of high tensile steel with a yield stress of 50 kgf/mm² with respect to stiffener spacing for different thicknesses. The average ultimate stress σ_{xu} of the 14 mm thick conventional steel plate is also plotted. These relationships are calculated from Eq. (9). **Figure 9** shows the ultimate strength per unit breadth ($\sigma_{xu}t$) of these plates plotted against the stiffener spacing.

A HTS plate (σ_o=50 kgf/mm²) of 12 mm thickness has an ultimate strength nearly equal to the original 14 mm steel plate for all frame spacing between 700 and 1000 mm and it has higher ultimate strength for smaller frame spacing.

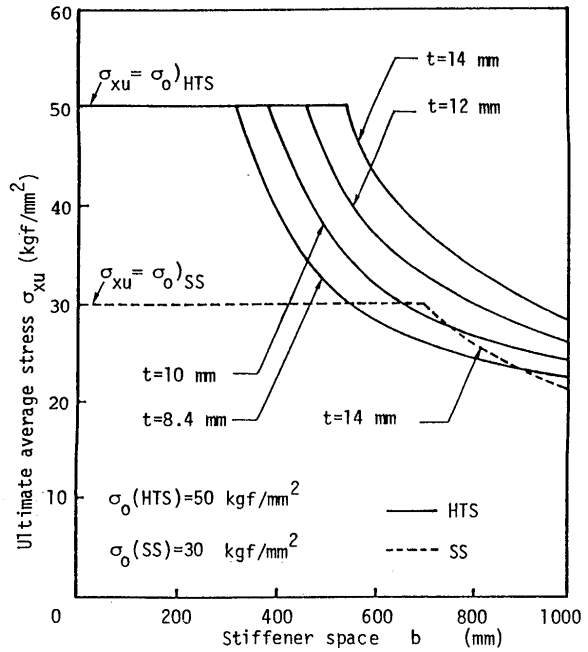

Fig. 8 Relationships of ultimate average stress to stiffener space

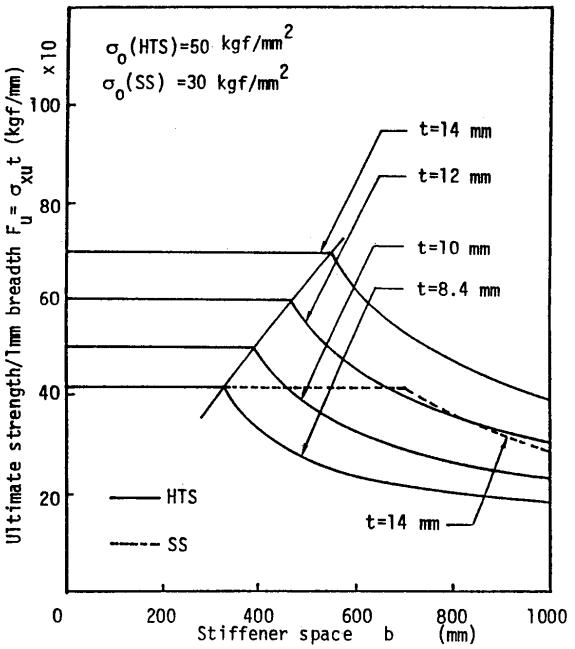

Fig. 9 Relationships of ultimate strength to stiffener space

Similar relationship for σ_o=80 kgf/mm² are shown in **Figs. 10 and 11**. A HTS plate of 9 mm thickness has an ultimate strength equal to that of the original steel plate at stiffener spacing equal to 1000 mm. While a 10 mm thick plate is necessary to carry the same load as that of the 14 mm conventional mild plate if b=700 mm.

6. Design Against Fatigue

Fatigue strength at a point of a structure is generally measured by the magnitude of the cyclic stress range S and a necessary number of cycles N (fatigue life) before a crack is produced at this point. Two approaches are available to assess the fatigue strength of structures, which are the S-N curve approach and the fracture mechanics approach. The S-N curve approach is simpler and more frequently used in the conventional design stage. In this paper, only this approach is applied.

6.1 Response to cyclic longitudinal in-plane loading

Let the panel shown in Fig. 1 be considered again. When the panel is subjected to a cyclic in-plane load in the form of uniform shortening and extension in x-direction (The direction of the stiffeners), the acting stress rang, S_x, at a point may be expressed as follows.

$$S_x = \sigma_c - \sigma_t \quad (15)$$

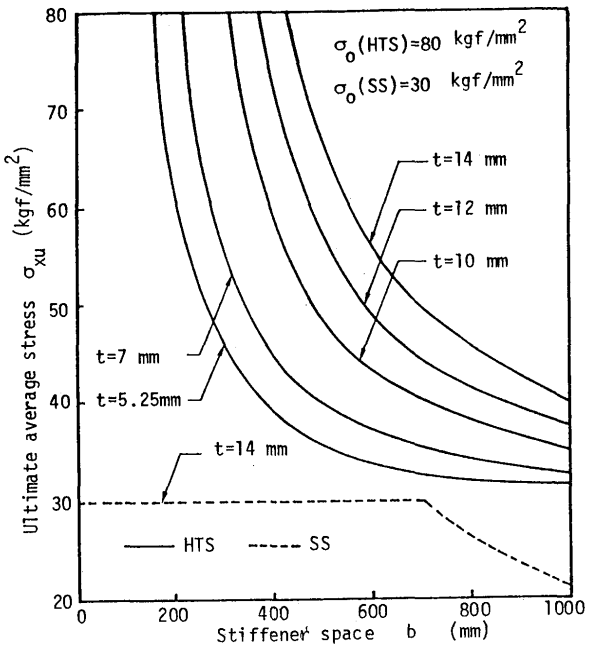

Fig. 10 Relationships of ultimate average stress to stiffener space

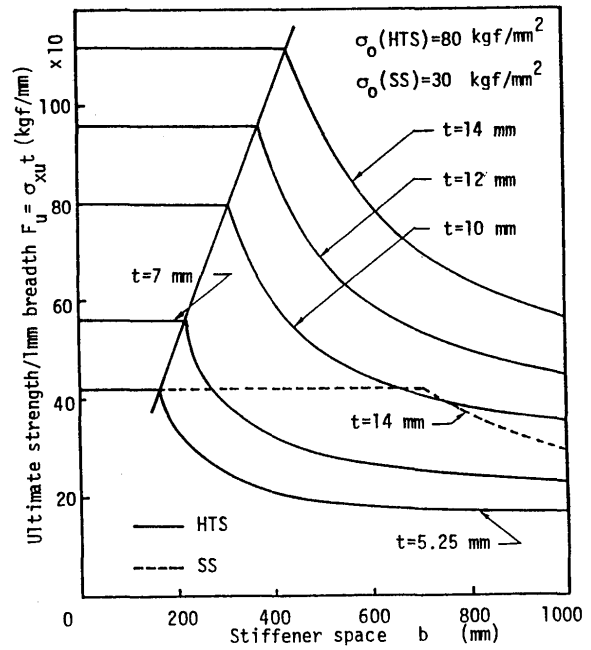

Fig. 11 Relationships of ultimate strength to stiffener space

where, σ_c is the peak compressive (positive) stress at this point and

σ_t is the peak tensile (negative) stress at the same point

Then, the mean stress may be expressed as

$$\sigma_m = (\sigma_c + \sigma_t)/2 \tag{16}$$

where, σ_m is positive when it is compressive.

These stresses are illustrated in **Fig. 12**, in the case of regular cyclic loading.

In the case where the peak compressive stress acting on the stiffened plate is smaller than the uniaxial buckling stress σ_{xcr} of the plate panel and the plate panel are assumed to be free from initial imperfection, the stress range, S_x, will be the same at any point in the plate. In this case, no stress in y-direction is produced since the longitudinal edges are free to move in the plane of plate.

On the other hand, if the peak compressive stress is higher than σ_{xcr}, the plate panels between the stiffeners will buckle. As mentioned before, the stress distribution is no longer uniform and become as shown in Fig. 2 with the peak maximum compressive membrane stress σ_{xmax} in x-direction is induced along the longitudinal edges of the plates (along the stiffeners) and is expressed in terms of σ_{xav} (the peak average compressive stress) as by Eq. (2). Notations "maximum" and "average" are used with respect to the plate breadth b, while terms "mean" and "peak" are used with respect to the elapse of time as indicated in Figs. 2 and 12. In this case, the acting stress range at a point on longitudinal edges of a plate panel may be expressed by the following equation.

$$S_{xmax} = \sigma_{xmax} - \sigma_t = 2\sigma_{xav} - \sigma_{xcr} - \sigma_t \tag{17}$$

and the mean stress may be given by

$$\sigma_{xm} = (\sigma_{xmax} + \sigma_t)/2 = (2\sigma_{xav} - \sigma_{xcr} + \sigma_t)/2 \tag{18}$$

In y-direction, the minimum (tension) membrane stress σ_{ymin} occurs in the middle of each half buckling wave and is given by Eq. (3). At the stiffeners, restraining moments are produced by the stiffeners resisting the rotation of the plate around its longitudinal edges as shown in **Fig. 13**. These moments are small and usually neglected when the buckling and post-buckling behaviors of the plate panels are dealt. However these moments cause high local stress

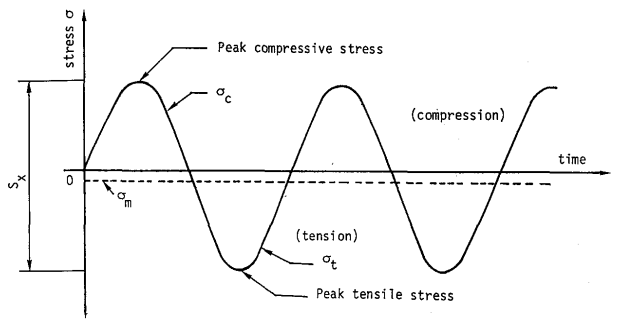

Fig. 12 Regular cyclic stress on a plate without buckling

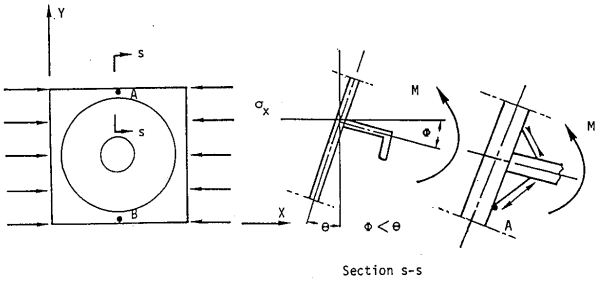

Fig. 13 Distortion of a stiffener induced by panel buckling

σ_{yb} in y-direction on the plate surface in the vicinity of the toe of the weld connecting the plate to the stiffener. This stress acts together with σ_{ymin} and is maximum at points such as A and B which are in the middle of each half buckling wave as indicated in Fig. 13. Although analytical evaluation of this stress is difficult, it may be expressed in the form as,

$$\sigma_{yb} = -\Psi(\sigma_{xav} - \sigma_{xcr})^{1/2} \tag{19}$$

The function Ψ depends on the plate dimensions, stiffener torsional stiffness and the size of the weld. The values of σ_{yb} and Ψ may be evaluated in each particular case using a numerical method such as a finite element method.

In summary, in the post-buckling stage, local cyclic stresses at points A and B are produced in two directions:

(1) The stress range in x-direction is referred to as the longitudinal stress range S_x and is given by Eq. (17).
(2) The stress range in y-direction is referred to as the transverse stress range S_y and is given by consideration of Eqs. (3) and (19). These two local cyclic stresses are illustrated in **Fig. 14**.

Since these cyclic stresses in x and y directions occur at the same position, some interaction may be expected. Experimental evaluation of S-N curves using specimens with representative geometries and loading conditions including two dimensional stress state is necessary for an accurate evaluation of fatigue behavior. In absence of such S-N curves, however, these two-dimensional cyclic stresses are treated separately in this study neglecting any interactions.

6.2 Fatigue due to random cyclic loading

In this section, the consequences of local buckling on fatigue behavior under random wave loading are considered. The Miner rules is used to evaluate damage factors, adopting the assumptions generally accepted. Necessary modifications are made in order to take account of buckling consequences.

6.2.1 Transfer function

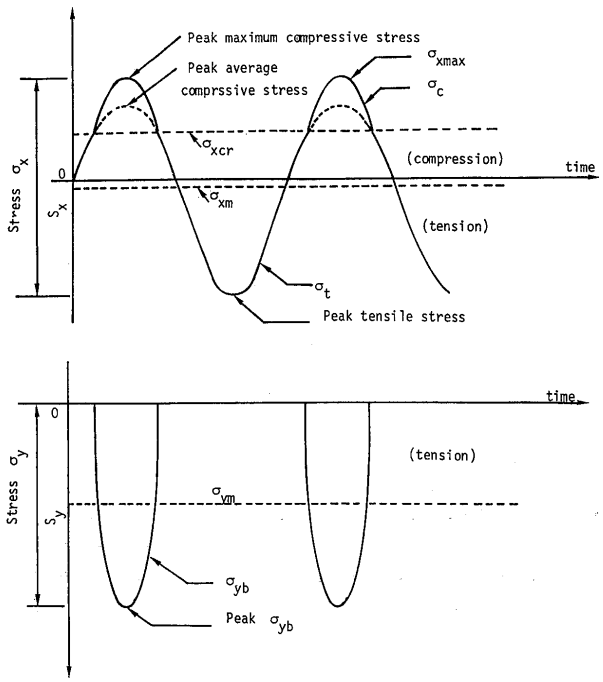

Fig. 14 Regular cyclic stress on a plate with buckling

Generally, a transfer function may be defined as the ratio of the stress response to the wave height. That is

$$T = S/H \tag{20}$$

where, T is the transfer function,
S is the stress range,
and, H is the wave height.

T is usually assumed to be constant, that is, a linear relationship between H and S is assumed as shown by a solid line in **Fig. 15**.

For the stiffened plate under consideration, the dimensions of the plate panel are assumed as such it will buckle at a wave height H_{cr} and the corresponding stress range is equal to S_{xcr},

$$S_{xcr} = \sigma_{xcr} - \sigma_t)_{Hcr} \tag{21}$$

For wave heights smaller than H_{cr}, the stress range in x-direction, S_x, will follow Eq. (20), where S_x is given by Eq. (15)

A transfer function, based on the stress range at H_{cr}, may be writtn as follows,

$$T_x = S_x/H = S_{xcr}/H_{cr} \tag{22}$$

Equation (22) assumes a linear relationship between S_x and H for $0 \leqq S_x \leqq S_{xcr}$.

For wave heights larger than H_{cr}, the average stress range in x-direction, S_{xav}, will follow Eq. (20) and

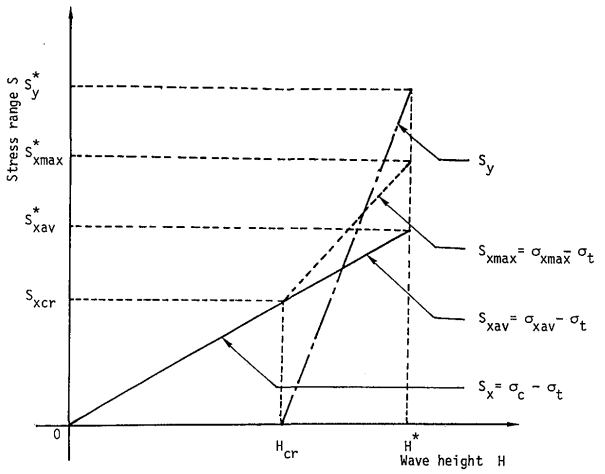

Fig. 15 Wave height-to-stress range transfer function

$$S_{xav} = \sigma_{xav} - \sigma_t \tag{23}$$

However, the stress range in x-direction at points A and B, S_{xmax}, as given by Eq. (17), will be higher than S_{xav}. For this post-buckling range, a transfer function $T'_x (= S_{xmax}/H)$ may be expressed as follows, based on the response at a wave with a probability of exceedance of 10^{-8},

$$T'_x = \{[\alpha(H - H_{cr}) + \sigma_{xcr}] - \sigma_t^*(H/H^*)\}/H \tag{24}$$

where, $\alpha = (\sigma_{xmax}^* - \sigma_{xcr})/(H^* - H_{cr})$

* refers to values at probability of exceedance of 10^{-8}

Equation (24) assumes a linear relationship between S_{xmax} and H for the range of loading between the buckling and the point of 10^{-8} probability of exceedance, as shown by the dashed line in Fig. 15. It is to be noted that σ_{xav} and S_{xav} after buckling are corresponding to σ_c and S_x before buckling.

In y-direction, the stress range S_y for wave heights larger than H_{cr} is given by consideration of Eqs. (3) and (19)

$$S_y = 0 - (\sigma_{yb} + \sigma_{ymin})$$

or
$$S_y = \Psi(\sigma_{xav} - \sigma_{xcr})^{1/2} + \sigma_{xav} - \sigma_{xcr} \tag{25}$$

As mentioned before Ψ may be evaluated from a non-linear finite element analysis. More directly, S_y at a wave of a probability of exceedance of 10^{-8} (S_y^*) may be evaluated by such a finite element analysis. Based on the response at a wave with a probability of exceedance of 10^{-8}, a transfer function T'_y may be expressed as follows

$$T'_y = S_y/H = S_y^*(H - H_{cr})/[(H^* - H_{cr})H] \tag{26}$$

Equation (26) assumes a linear relationship between S_y and H for the range of loading between the buckling and the point of 10^{-8} probability of exceedance, as shown by the dash-dot line in Fig. 15.

6.2.2 The probability density function

Generally, the Weibull or the exponential probability density function is used to represent the stress response based on a linear tansfer function. In this paper the exponential probability density function is adopted.

$$P(S) = (1/\lambda)e^{-S/\lambda} \tag{27}$$

where, $P(S)$ is the exponential probability density function,

S is the nominal stress range,

and, λ is the scale parameter of this function.

The probability that the stress range S^* is reached or exceeded during the total numbers of cycles $N^*(=10^8)$ is given as follows

$$P'(S^*) = \int_{S^*}^{\infty} P(S)dS = 1/N^* \tag{28}$$

From which, λ may be evaluated as follows

$$\lambda = S^*_x / ln\ N^* \quad \text{in case of } H^* < H_{cr} \tag{29}$$

$$\lambda = S^*_{xav} / ln\ N^* \quad \text{in case of } H^* > H_{cr} \tag{30}$$

Equation (28) is represented by the solid lines in **Figs 16-a** and **16-b**.

Let the dimensions of the plate panels be such that buckling occurs at a certain stress range, S_{xcr}. For stress ranges larger than S_{xcr}, the probability density distribution of the average stress range S_{xav} as defined by Eq. (23) will follow Eq. (27). However, S_{xmax}(given by Eq. (17)) will be larger than S_{xav} and may be represented by the dashed line in Figs. 16-a and 16-b. The probability of exceedance of any S_{xmax} at any wave height is equal to the probability of exceedance of S_{xav}(which produces this S_{xmax}) at this wave height.

In y direction, S_y is given by Eq. (25) and represented by the dash-dot line in Figs. 16-a and 16-b. Here, also the probability of exceedance of any S_y at any wave height is equal to the probability of exceedance of S_{xav} (which produces this S_y) at this wave height.

6.2.3 Miner's damage factor

Miner's damage factor D may be expressed as follows,

$$D = \int_0^{\infty} dn/N \tag{31}$$

where, dn is the number of cycles at a stress range S

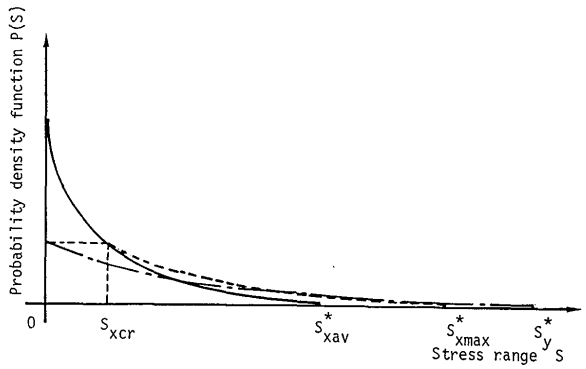

Fig. 16-a Probability density distribution of S_x and S_y.

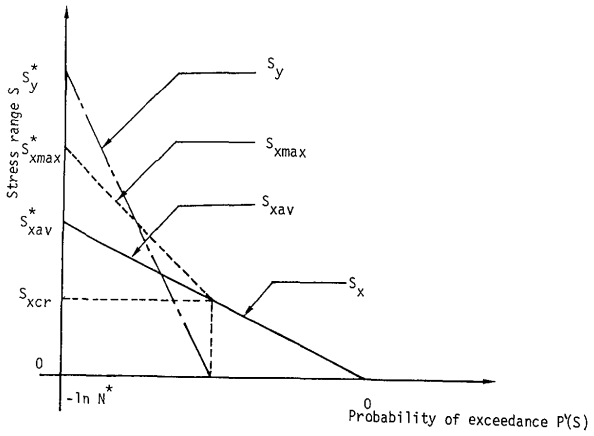

Fig. 16-b Probability of exceedance S_x and S_y.

and, N is the number of cycles at failure under this stress range S.

dn may be expressed as follows

$$dn = (N^*/\lambda)e^{-S/\lambda}\, dS \tag{32}$$

while N may be expressed using an S-N curve as follows

$$N = C\ S_r^{-m} \tag{33}$$

where, C is the value of N at the intersection of the S-N curve with the log N axis as shown in **Fig. 17**.

m is the inverse negative slope of the S-N,

and, S_r is the actual stress range acting at a point, under a nominal stress range equal to S.

Substituting Eqs. (32) and (33) into Eq. (31), D may be expressed as follows,

$$D = N^*/C \int_0^\infty (S_r^m/\lambda)e^{-S/\lambda}\, dS \tag{34}$$

First, the damage factor D_x due to the longitudinal stress range at point A or B is considered. Since the stress is represented by a bi-linear function (Eq. (22) for $0 \leqq S_x \leqq S_{xcr}$ and Eq. (24) for $S_{xcr} \leqq S_{xav} \leqq S_{xav}^*$ i.e. $S_{xcr} \leqq S_{xmax} \leqq S_{xmax}^*$). Equation (34) may be written for the longitudinal stress range as follows,

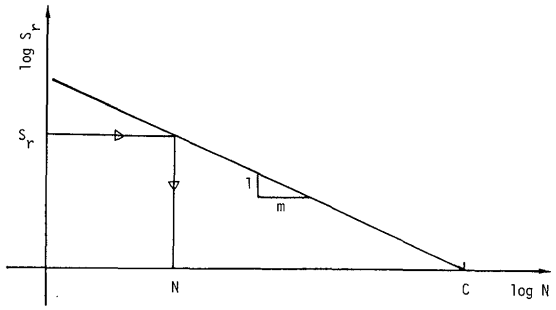

Fig. 17 Schematic representative of S-N curve

$$D_x = N^*/C\{\int_0^{S_{xcr}} (S_x^m/\lambda)e^{-S/\lambda}\, dS + \int_{S_{xcr}}^\infty (S_{xmax}^m/\lambda)e^{-S/\lambda}\, dS\} \tag{35}$$

Equation (35) may be rearranged and written as follows

$$D_x = N^*/C\{\lambda^m \Gamma(1+m)+q\} \tag{36}$$

where, Γ is the Gamma function,

and, $$q = \int_{S_{xcr}}^\infty ([S_{xmax}^m - S_{xav}^m]/\lambda)\ e^{-S_{xav}/\lambda}\, dS_{xav} \tag{37}$$

q may be evaluated by numerical integration. Equation (17) may be used to evaluate S_{xmax}. The upper limit of integration may be taken equal to S_{xav}^* without any appreciable error.

The damage factor D_y of the transverse stress range S_y may be similarly evaluated from Eq. (34). Since the value of S_y is equal to zero in the pre-buckling range, the integration is taken between the point of buckling and infinity.

$$D_y = N^*/C \int_{S_{xcr}}^\infty (S_y^m/\lambda)e^{-S_{xav}/\lambda}\, dS_{xav} \tag{38}$$

S_y may be expressed as follows

$$\begin{aligned} S_y &= S_y^*(S_{xav} - S_{xcr})/(S_{xav}^* - S_{xcr}) \\ &= \Phi(S_{xav} - S_{xcr}) \end{aligned} \tag{39}$$

D_y may then be obtained as,

$$D_y = N^*/C \int_{S_{xcr}}^\infty \Phi^m([S_{xav} - S_{xcr}]^m/\lambda)\ e^{-S_{xav}/\lambda}\, dS_{xav} \tag{40}$$

The integration in Eq. (40) may be performed numerically. Similarly, the upper limit of integration may be taken equal to S_{xav}^* without any appreciable error.

6.3 Design procedure and numerical results

Equations (36) and (40) may be used to produce design graphs. Due to many variables involved in these two equations, however, too many design graphs would be necessary. It may be more convenient to use these equations directly to evaluate damage factors and compare them with allowable values (usuall $\leqq$ 1.0). A procedure to evluate the damage factors D_x and D_y in x- and y-directions respectively is outlined in **Fig. 18** and may be summarized as follows.

1. Calculate the longitudinal compressive and the tensile stresses σ_c^* and σ_t^* acting on the considered panel under a load with a probability of exceedance of 10^{-8} Then, evaluate the stress range under this load

$$S_x^* = \sigma_t^* - \sigma_t^* \tag{41}$$

2. Compare σ_c^* with σ_{xcr}, the buckling stress of plates between stiffeners. If $\sigma_t^* \leqq \sigma_{xcr}$, no buckling is expected, and the fatigue life may be checked, if necessary, in the conventional way.
3. In the case where $\sigma_c^* > \sigma_{xcr}$, buckling is expected. $\sigma_t)_{Hcr}$, the tensile stress, induced by the same wave height as σ_{xcr} may be evaluated as follows assuming a linear transfer function,

$$\sigma_t)_{Hcr} = \sigma_t^*(\sigma_{xcr}/\sigma_c^*) \tag{42}$$

4. S_{xcr} appearing in Eqs. (37) and (40) is evaluated as given in Eq. (21).
5. Evaluate q using Eq. (37) by numerical integration (using Simpson's rule for example).
6. Evluate D_x using Eq. (36).
7. Perform a nonlinear finite element analysis to evaluate S_y^*, the stress in y-direction at the weld toe in the middle of half buckling waves, under a load with a probability of exceedance of 10^{-8}. An example of such an analysis may be found in Ref. 3).
8. Evaluate Φ, that is
   $\Phi = S_y^*/(S_x^* - S_{xcr})$
9. Evaluate D_y using Eq. (40) by numerical integrations.
10. Check D_x and D_y against their allowable values and modify the structure, and reanalyse if necessary.

Figure 19 shows the damage factor due to the longitudinal stress range for different plate thicknesses and frame spaces. In this figure, the loads per unit breadth of plates (S^*t) are kept constant. S^*t of a plate 14 mm thick is taken equal to 20 kgf/mm². S-N curve of class D from DNV[4] is adopted with $C = 10^{12.18}$ and $m=3$. It may be seen that the damage factor for each plate thickness does not change substantially (in this range of thickness and frame space) with the change of frame spaces. This indicates that buckling effect on fatigue damage in this range of

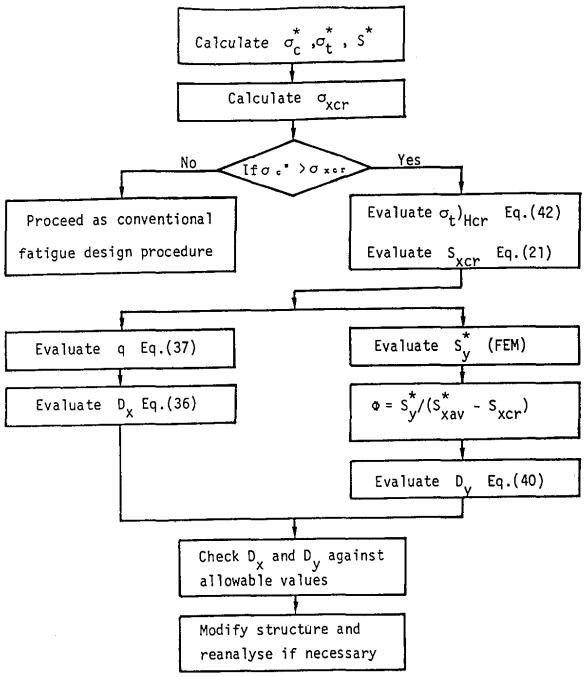

Fig. 18 Flow chart of fatigue design procedure

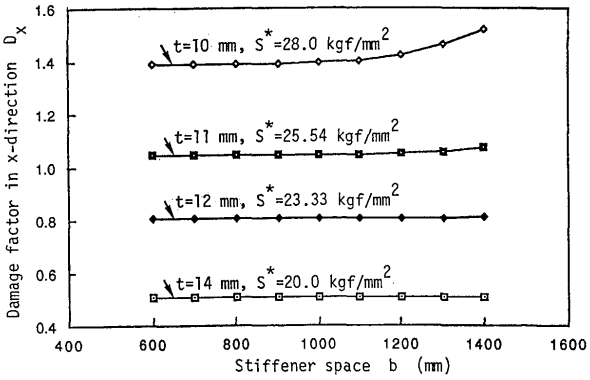

Fig. 19 Damage factor D_x against stiffener space (S-N curve of class D from DNV)

thickness and frame space is not appreciable. On the other hand, the damage factor increases substantially as the plate thickness decreases. This is due to the higher stress range S^* developed in thinner plates in order to carry the same loads as thicker ones.

In **Fig. 20**, the damage factor due to the transverse stress range is plotted for different plate thicknesses and frame spaces. Here also, (S^*t) is kept constant, and S^* is taken equal to 20 kgf/mm² for a plate 14 mm thick. S-N curve of class F from DNV is used with $C = 10^{11.8}$ and $m=3$. σ_y^* is calculated using a value of $\Psi=6$ (see Eq. (19)) which is evaluated from a practical case. It may be seen that damage factors for plate thicknesses more that 8 mm become negligibly small and those for thinner plates (where S_{xcr} is small) become larger.

When a different S-N curve[3] with $C=10^{18.65}$ and $m=6$

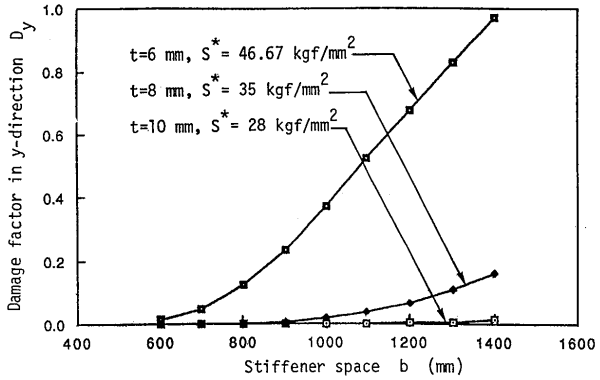

Fig. 20 Damage factor D_y against stiffener space (S-N curve of class F from DNV)

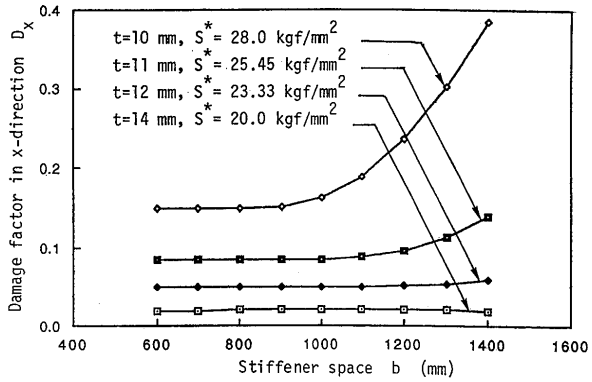

Fig. 21 Damage factor D_x against stiffener space(S-N curve from Ref.3)

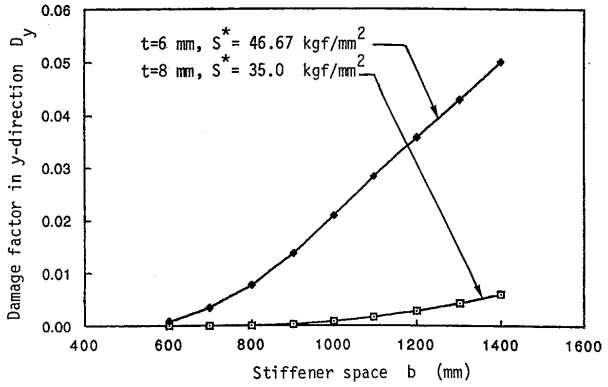

Fig. 22 Damage factor D_y against stiffener space(S-N curve from Ref. 3)

is adopted, damage factors calculated under similar assumptions are plotted in **Figs. 21** and **22**.

Figures 23 and **24** show the damage factor for different plate thicknesses and different loads per unit breadth of plates using *DNV's* curves D and F respectively. Appreciable increase of damage factors for the transverse stress range S_y may be observed with thin plates in the range of

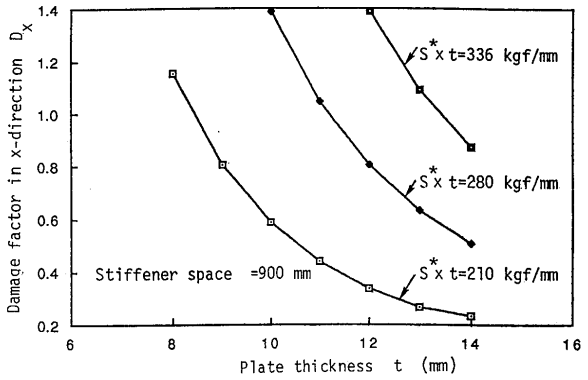

Fig. 23 Damage factor D_x against plate thicknesses for different levels of cyclic loading (S-N curve of class D from DNV)

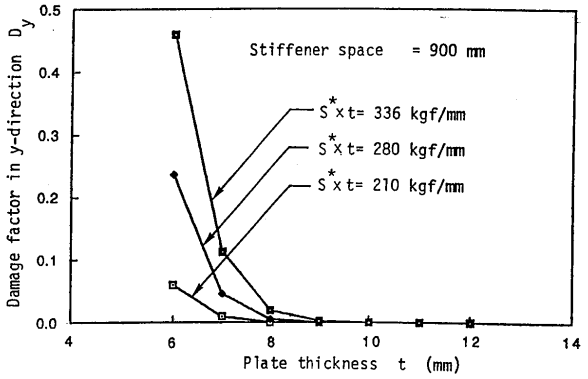

Fig. 24 Damage factor D_y against plate thicknesses for different levels of cyclic loading (S-N curve of class D from DNV)

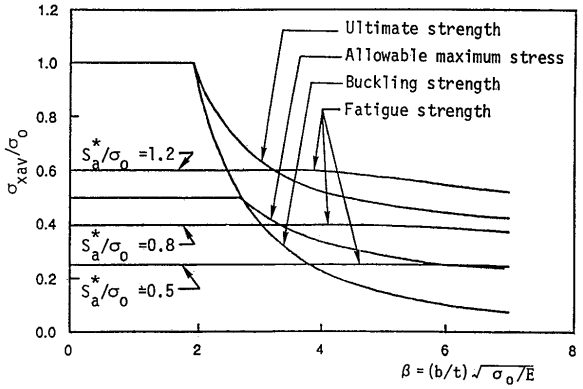

Fig. 25 relationship of allowable stress to plate slenderness ratio β

thickness being smaller than 5 or 6 mm.

The allowable average stresses are calculated based on the three criterion described in this paper, and they are plotted against the plate slenderness ratio β in **Fig. 25**. Ultimate compressive strength and allowable maximum stress criteria are to be used to compare high tensile steel panels with comventional mild steel ones. The allowable average compressive stresses are calculated with respect to

the fatigue criterion (damage factor $D_x=1$) under a longitudinal stress range S_x assumed as being $\sigma_c^*=-\sigma_t^*$, using S-N curves which are furnished for $m=3$ and $S_a^*/\sigma_o=0.5$, 0.8 and 1.2. Denoting S_R as the allowable stress range of the material corresponding to a fatigue life of 10^8 cycles, S_a^* is expressed as

$$S_a^*=S_R \ ln\ N^*/[\Gamma(1+m)]^{1/m}=S_R\ \xi$$
$$(\xi=10.13 \text{ for } m=3)$$

In constructing this graph, the effect of the interaction between the longitudinal and the transverse stresses is not taken into account. This effect needs to be clarified by further experimental and theoretical studies.

It may be seen also from this figure that buckling has only a little effect on fatigue for plates with slenderness ratio up to 6 or 7.

It is to be noted that effects of initial deflection of plates and welding residual stresses in the stress range above buckling are not included in the above results. These will lead to some increase of the damage factors. These effects will be investigated and the results be reported in future publication.

7. Conclusions

In this paper, three subjects associated with buckling accepted design applied to ship structures are discussed. Namely, maximum stress, ultimate strength and fatigue under regular and random loads. A design philosophy is proposed. Design criteria, design methods, design graphs and relevant equations are presented in connection with these subjects. Numerical examples are also presented.

From these graphs and numerical results, the following conclusions may be drawn.

1. The use of high tensile steels may make it possible to reduce plate thickness substantially, satisfying the current design and safety criteria such as maximum allowable stress and ultimate strength of plates.
2. Buckling may have only negligible effects on fatigue strength of perfectly flat rectangular plates being thicker than 8 mm. Effects of initial deflection and residual stresses on fatigue need to be investigated to check the validity of this conclusion with actual ship plates.

In this study, the effect of the interaction of the longitudinal and the transverse stress ranges is not taken into account. This effect should be clarified by further experimental and theoretical studies, since the effect may affect the conclusion mentioned above.

Acknowledgment

This research is supported by Ministry of Education, Science and Culture, through the Grand-in-Aid for scientific research.

References

1) Hori, T., Sekihama, M. and Rashed, S. M. H., "Structural 'Design-by-Analysis' Approach Applied to A Product Oil Carrier with Uni-directional Girder System", RINA, Spring Meeting, 1990.

2) Ueda, Y., Rashed, S. M. H. and Paik, J. K., "Plate and Stiffened Plate Units of The Idealized Structural Unit Method(1st report)", J1 of Soc. of Naval Architecture of Japan, Vol. 156, 1984 (in Japanese)

3) Ueda, Y., Tomita, Y. Umezaki, K., Mizuno, H., Kawamoto, Y., Nishimura, S. and Kusuba, S., "Post Buckling Design of Very Thin Stiffened Panels unde rCyclic Axial Loading (1st report)", J1, Soc. of Naval Architecture of Japan, Vol. 170, 1991 (in Japanese)

4) Almar-Naess, A., "Fatigue Handbook", Offshore Steel Structure, Published by Tapir, Norway, 1985